Interferometric Imaging of Hydrogels Undergoing Volume Changes

Yunmei Xu and Iwao Teraoka*

Herman F. Mark Polymer Research Institute, Polytechnic University, 333 Jay Street, Brooklyn, New York 11201

Received February 23, 1999; Revised Manuscript Received May 13, 1999

ABSTRACT: A polyacrylamide hydrogel undergoing a volume change was studied by using interferometric imaging. The method produces the radial distribution of the matrix density for the cylindrical hydrogel at different times during the volume transition caused by solvent change. When the water-swollen gel was immersed in a water−methanol mixture, contraction of the gel matrix occurred first in the edge and propagated to the center. The edge did not reach the equilibrium density immediately after the solvent change. The gel contracted rather evenly, although the edge maintained a higher density during the change. After reaching the uniform density, the center of the gel contracted further whereas the edge remained unchanged. A similar pattern was observed in the reswelling in pure water. These findings indicate that the gel studied had a shear modulus not small compared with its bulk modulus.

Introduction

The volume transition of a hydrogel in response to a change of solvent composition has been intensively studied in the past two decades.[1] In these studies, the equation of state for the gel was derived to account for the observed continuous and discontinuous volume phase transitions.[2] The past studies focused on the critical behavior,[3−5] static and dynamic properties in the swollen and shrunk states,[6−9] and the swelling and deswelling kinetics. In the studies of the latter, visual inspection including optical microscopy,[5,10] fluorescence spectroscopy,[11] and NMR[12] were employed. It was shown that the change in the diameter of spherical and cylindrical gels agrees with the change described by collective diffusion of the gel matrix.[13] Each of the techniques has its own advantages, but none of them give the density profile of the gel matrix as a function of the radial distance from the center. Information on the density profile will be valuable in elucidating the mechanism of the transition. Many questions need to be answered: how the solvent is transferred during the volume change,[14,15] how microscopic instability evolves into an overall structural change,[16−18] etc.

In this report we show how the interferometric imaging technique can be applied to studies of hydrogels undergoing structural changes such as volume transitions. Immersion of a water-swollen gel into a solution or a less favorable solvent can cause the change, for instance. Earlier Dube and Teraoka[19] used the Jamin interferometry to study infusion of polymer chains into a solid porous silica bead. The spatial resolution of the method allowed them to identify whether entrance of the chains into the pore openings on the bead surface or diffusion of the chains through the tortuous pore structure determines the overall rate of infusion.

The digital image analysis of interferograms coupled with deconvolution, when applied to a hydrogel, can measure the local density variation of the gel matrix and/or the local concentration of a penetrant within the gel. The in situ, nondestructive measurement utilizes a difference in the refractive index between the solvent and the gel matrix (or the penetrant). Therefore, there is no need to label the gel matrix or the penetrant unlike magnetic resonance imaging,[20−25] electron spin resonance imaging,[26,27] or fluorescence microscopy. The spatial resolution is limited by the wavelength of light or ∼1/1000 of the gel dimension, whichever is larger. The latter is due to a finite number of pixels of the image-capturing device used.

Our interferometric imaging technique takes advantage of close index matching between water (n_D^{20} = 1.3330) and methanol (n_D^{20} = 1.3290) and the vastly different refractive index of the gel matrix (n_D^{20} = 1.5945 for polyacrylamide). Water is a good solvent for the gel. When methanol is added to the surrounding fluid and the fluid within the gel is exchanged by diffusion, its refractive index barely changes, although its interaction with the gel matrix changes greatly, forcing contraction. Then it is possible to observe how the gel matrix deforms without being disturbed by a spatially and temporally drifting refractive index of the permeating fluid.

First we explain how the interferometric imaging can be applied to the study of hydrogels. Then we present examples of images and the results of image analysis for a deswelling process in which a water-swollen gel was immersed in a water−methanol mixture. We will also show the results for the reswelling process in which the partially shrunk gel was swelled in water.

Jamin Interferometry of a Cylindrical Medium

In the Jamin interferometer,[19,28] two near-parallel laser beams split from a single beam of wavelength λ intersect to interfere. They are projected onto a screen to produce an interference pattern that consists of sinusoidally modulated parallel fringes. When one of the beams illuminates a small medium with a uniform refractive index n_I different from the index n_E of its surrounding the other beam travels, the interference fringe pattern is displaced for the portion of light that has traveled in the medium. Figure 1 illustrates the fringe pattern for a cylindrical medium of diameter $2a$. An $x-y$ coordinate system is set up for the convenience of the image analysis. The y-axis is along the center axis of the gel image. The background fringes have a period ξ_x measured along the x-axis and a slope of k. They are represented by

$$y = kx + b + mk\xi_x \quad (1)$$

10.1021/ma990261x CCC: $18.00
Published on Web 06/11/1999

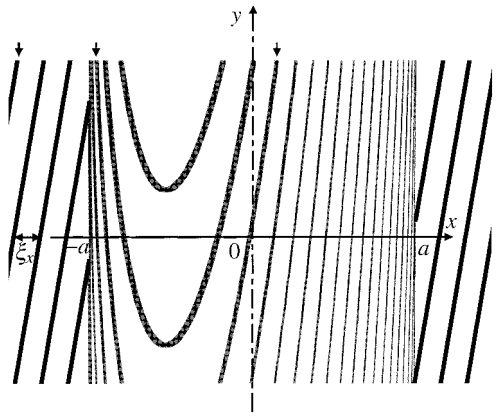

Figure 1. Schematic of the interferogram for a uniform cylindrical medium.

where b is a constant and m is an integer. The contour equation for the fringe within the medium is

$$y = bk + b + k\xi_x[m - 2\sqrt{a^2 - x^2}(n_I - n_E)/\lambda] \quad (2)$$

The difference between n_I and n_E distorts the pattern within the gel image into near-elliptic arcs. When $|k|$ is large, i.e., the background fringes are nearly parallel to the cylinder, the trace of each interior fringe is close to a parabola with its axis near the edge of the cylinder. When $|k|$ is small, in contrast, the axis of the parabolas runs near the axis of the cylinder. Each interior fringe is associated with one of the parallel fringes in the background image or those hidden by the gel image. For instance, the two interior fringes indicated by the arrows share m with the exterior fringe indicated by the arrow. We focus here on how much the x-intercept of each fringe within the gel, x_1, is displaced with reference to the intercept of the corresponding background fringe. The ratio of the displacement Δx to ξ_x is an invariant of ξ_x and k. The plot of $\Delta x/\xi_x$ as a function of x_1 will be on a semiellipse:

$$\Delta x/\xi_x = (2a/\lambda)(n_I - n_E)[1 - (x_1/a)^2]^{1/2} \quad (3)$$

and maximizes for a fringe at $x_1 = 0$. This equation is the same as the one obtained for a spherical medium, because the cross section is circular in both media.

When the gel is not uniform, it will produce spatial variations in n_I. Then the plot of $\Delta x/\xi_x$ will deviate from the semiellipse. The photon that images at x_1 travels a chord of length of $2l = 2(a^2 - x_1^2)^{1/2}$ in the circular cross section of the gel. Therefore, n_I in eq 3 for the fringe at x_1 is the average refractive index along the chord:

$$\overline{n_I}(x_1) = l^{-1}\int_0^l n_I((x_1^2 + y^2)^{1/2})\, dy \quad (4)$$

where axial symmetry is assumed for the gel. To convert $\overline{n_I}(x_1)$ into $n_I(r)$, deconvolution is needed. Typically, a polynomial consisting of even-order terms only is used.[19] If

$$n_I(r) - n_E = \sum_{n=0}^{N} \zeta_{2n}(r/a)^{2n} \quad (5)$$

then

$$\overline{n_I}(x_1) - n_E = \sum_{l=0}^{N} \xi_{2l}(x_1/a)^{2l} \quad (6)$$

where

$$\xi_{2l} = \sum_{n=1}^{N} \zeta_{2n} \frac{(2n)!!}{(2n-2l)!!} \frac{(2n-2l-1)!!}{(2n+1)!!} \quad (7)$$

where $(2n)!! = (2n)(2n-2)\cdots 2$ and $(2n+1)!! = (2n+1)(2n-1)\cdots 1$.

A volume change of the gel forces both $2a$ and n_I to change. To obtain $\overline{n_I}(x_1) - n_E$ in eq 3 from the interferogram analysis, we need to know $2a$ for each image of the gel recorded. Fitting $\overline{n_I}(x_1) - n_E$ by eq 6 with a selected N gives ξ_{2l} for $l = 0, ..., N$. Then eq 7 gives ζ_{2n} for $n = 0, ..., N$, and $n_I(r) - n_E$ can be obtained as a function of r.

The refractive index $n_I(\mathbf{r})$ at $\mathbf{r}$ within the gel is given as

$$n_I(\mathbf{r}) = n_W + \frac{dn}{dc_G} c_G(\mathbf{r}) \quad (8)$$

where n_W is the refractive index of water, c_G is the gel matrix concentration, and dn/dc_G is the differential refractive index of the gel matrix in water. In our surrounding fluid of water−methanol, $n_W \cong n_E$. Then the refractive index profile is proportional to the gel density profile.

Experimental Section

Solvents. Methanol of ACS reagent grade from Brand-NU Laboratories was used as received. It was found that this grade of methanol has a refractive index closer to that of water compared with other grades of methanol that may contain impurities. This methanol alone had a refractive index smaller than that of water, in agreement with the values listed in the catalogues of the chemical suppliers. We could have used other grades of methanol, although the image analysis would become slightly more tedious. A small amount of the impurities, if any, will not change the characteristics of the volume change. Water was obtained from a water purifier, Easypure UV (Barnstead).

Synthesis of Polyacrylamide Gel. Polyacrylamide (PAAm) gel was prepared by free-radical polymerization following the standard procedure.[13] Acrylamide (0.5 g); *N*,*N*′-methylenebis-(acrylamide) (6.6 mg), the cross-linking agent; *N*,*N*,*N*′,*N*′-tetramethylethylenediamine (24 μL), the accelerator; and ammonium persulfate (4 mg), the initiator, were dissolved in deionized, degassed, and nitrogen-saturated water at 0 °C to a final volume of 10 mL. The solution was then transferred into octyldimethylchlorosilane-treated glass capillary tubing (interior diameter, i.d., was 0.78 mm for tubing from Warner Instrument; i.d. was 1.1−1.2 mm for tubing from Fisher Scientific), where gelation occurred at room temperature within several minutes. The gels were left in the tubes for 2 h and then immersed in methanol. The gels shrunk and became whitish in methanol. Then the gels were removed from the capillary and cut into pieces of a desired length. One of the gel pieces was inserted into the hole of a Teflon base and placed in a fluorometer cell (UVONIC type 23; 10 mm × 10 mm base) filled with water. The piece of gel restored its cylindrical shape, as shown later, and swelled to a diameter larger than the i.d. of the capillary tubing used to synthesize the gel. The diameters were approximately 1.4 and 1 mm for gels prepared in the 1.1 and 0.78 mm i.d. capillary tubings, respectively.

Interferometric Imaging System. A Jamin interferometer constructed earlier[19,28] was used here with a slight modification. A collimated laser beam (632.8 nm, 5 mW) is transformed into a slightly expanding beam (diameter ≅ 1 mm) by a lens. A beam displacer (a single crystal of calcite) splits

the beam into two parallel beams separated by about 4 mm. The cylindrical gel (diameter ca. 1−1.4 mm, length 1.5 cm) is held nearly vertically in the fluorometer cell filled with water or a water−methanol mixture. One of the beams illuminates a part of the gel whereas the other beam travels the surrounding fluid. The two beams are coupled by another beam displacer. The fringe pattern thus formed is magnified by a pair of convex lenses and projected onto a screen. The image is captured by a camcorder (Sony, CCD-FX710) connected to a Macintosh Quadra 660AV. Its built-in frame grabber records the image in a 640 × 480 pixel format. The image is analyzed with public-domain image analysis software "NIH-Image" (available at http://rsb.info.nih.gov/nih-image/).

The fluorometer cell is held in a cuvette holder (Milton Roy) with a water channel running through it. The temperature of the cell is maintained at 25.0 ± 0.1 °C by water circulating from a refrigerating bath. The cuvette holder is mounted on two translation stages with a micrometer to position the hydrogel at the optimal position with respect to the two beams and also to measure the diameter of the gel.

Measurement of Differential Refractive Index. A small differential refractive index of the methanol in water at 25.0 °C and $\lambda = 632.8$ nm was measured by using the interferometric imaging system. For this purpose, an NMR test tube (Kontes 897840-0000; i.d. = 2.40 mm; wall thickness = 0.28 mm; cut to a length of 55 mm) was firmly fixed in an open-top fluorometer cell (UVONIC type 3; 10 mm × 10 mm base) by two Teflon pieces. The cell was held tightly in the cell holder. Water was poured into the cell surrounding the tube. The NMR tube contained either water or a methanol solution of a known concentration. The existing solution in the NMR tube was withdrawn by using a syringe with a flexible Teflon tubing (o.d. = $^1/_{16}$ in.) to be exchanged for the next solution of a different concentration. Attention was paid not to apply excess force onto the tube or the cell during the exchange. For each concentration, the fringe pattern formed within the NMR tube was captured and analyzed in a procedure similar to our regular analysis method explained earlier. The liquids used to fill the NMR tube were pure water and 5.12, 8.04, 12.16, 15.10, and 19.04 wt % solutions of the methanol in water. From the shift in the fringe positions with increasing methanol concentration, dn/dw was estimated as −0.001 55, where w is the mass fraction of methanol in the solution. Details are explained in ref 29.

Diameter Measurement. A straight line parallel to the edge of the gel was marked on the projection screen. The translation stage was adjusted so that the marker line overlaps with one of the edges on the projection screen, and the micrometer reading was obtained. Then the cell holder was moved horizontally to overlap the marker line with the other edge of the gel image, followed by reading of the micrometer. The diameter of the gel was calculated by taking the difference of the two readings.

Results and Discussion

PAAm Gel in Water. Figure 2 shows a typical fringe pattern for an image of a cylindrical PAAm gel immersed in pure water. The pattern is similar to the one shown in Figure 1 except that a negative k inverted the pattern. A 10-pixel-wide rectangular bar perpendicular to the gel axis was selected as shown in the figure to draw the intensity profile plot (black = 255, white = 0). The positions of the dark and bright fringes were obtained in the plot. Figure 3 is a plot of $\Delta x/\xi_x$ for the dark fringes (closed circles) and the bright fringes (open circles). The solid line is the best fit by a semiellipse. The good fitting demonstrates that the gel matrix concentration was uniform and the cross section was circular, after the gel shrunk in methanol to be taken out from the glass capillary and reswelled in water to a different diameter. From $2a = 1.378$ mm and the peak value of $\Delta x/\xi_x$, we obtain $n_I - n_W = 4.02 \times 10^{-3}$. With

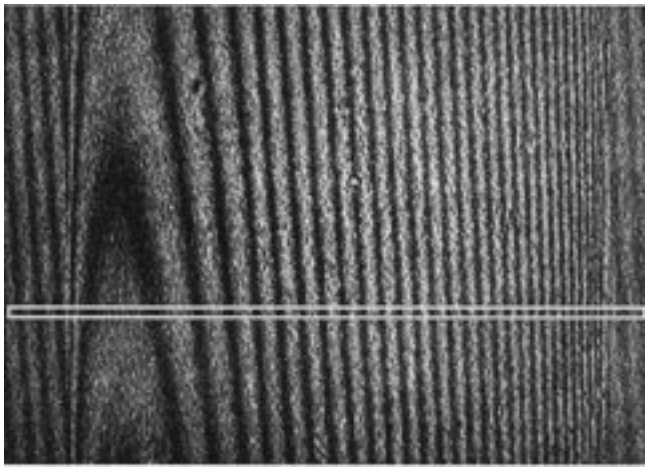

Figure 2. A typical interferogram of a PAAm gel in water. A white-outlined bar was selected for the intensity profile plotting.

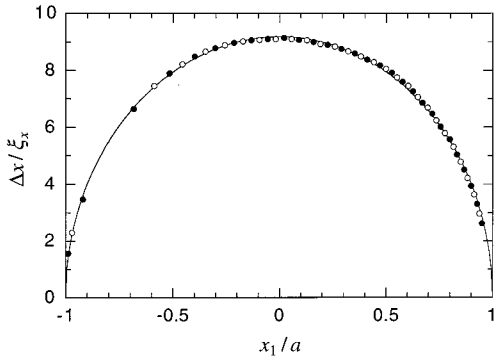

Figure 3. Plot of the relative displacement, $\Delta x/\xi_x$, as a function of the fringe intercept, x_1, obtained for the image shown in Figure 2. Filled and open circles represent the dark and bright fringes, respectively. The solid line is the best fit by a semiellipse.

dn/d$c_G = 0.182$ mL/g[30] for a solution of linear polyacrylamide at $\lambda = 632.8$ nm, c_G is estimated as 0.0221 g/mL. This value agrees with an estimate obtained from the volume (17.23 μL) of the swollen gel and its dried mass (0.39 mg).

Image Analysis of Deswelling and Reswelling. Another piece of cylindrical PAAm gel was fixed at the center of a fluorometer cell filled with water. A pair of interferograms, one for the image of the gel and the other for the background, were recorded at 25.0 °C. The diameter was also measured. Then, the exterior solvent was replaced with a water−methanol mixture (25 wt % of methanol) that had been sitting in another cuvette at 25.0 °C. The interferograms were recorded, and the diameter was measured at various times that followed. The time interval was as short as 2 min. Some of the interferograms taken before the solvent change (0 min) and in 15 min, 60 min, and 2 days after the change are shown in Figure 4. The diameter decreased, and the fringes became more condensed as time progressed.

Selected interferograms were analyzed with "NIH-Image". The displacement plots are shown in Figure 5 for the images recorded before the solvent change (0 min) and in 3 min, 8 min, 15 min, 40 min, 80 min, 187 min, 475 min, and 3 days after the solvent change. Fitting by a semiellipse is also shown. The relative displacement gradually increased, although the gel diameter decreased. The increase in $\overline{n_I}(x_1)$ was more

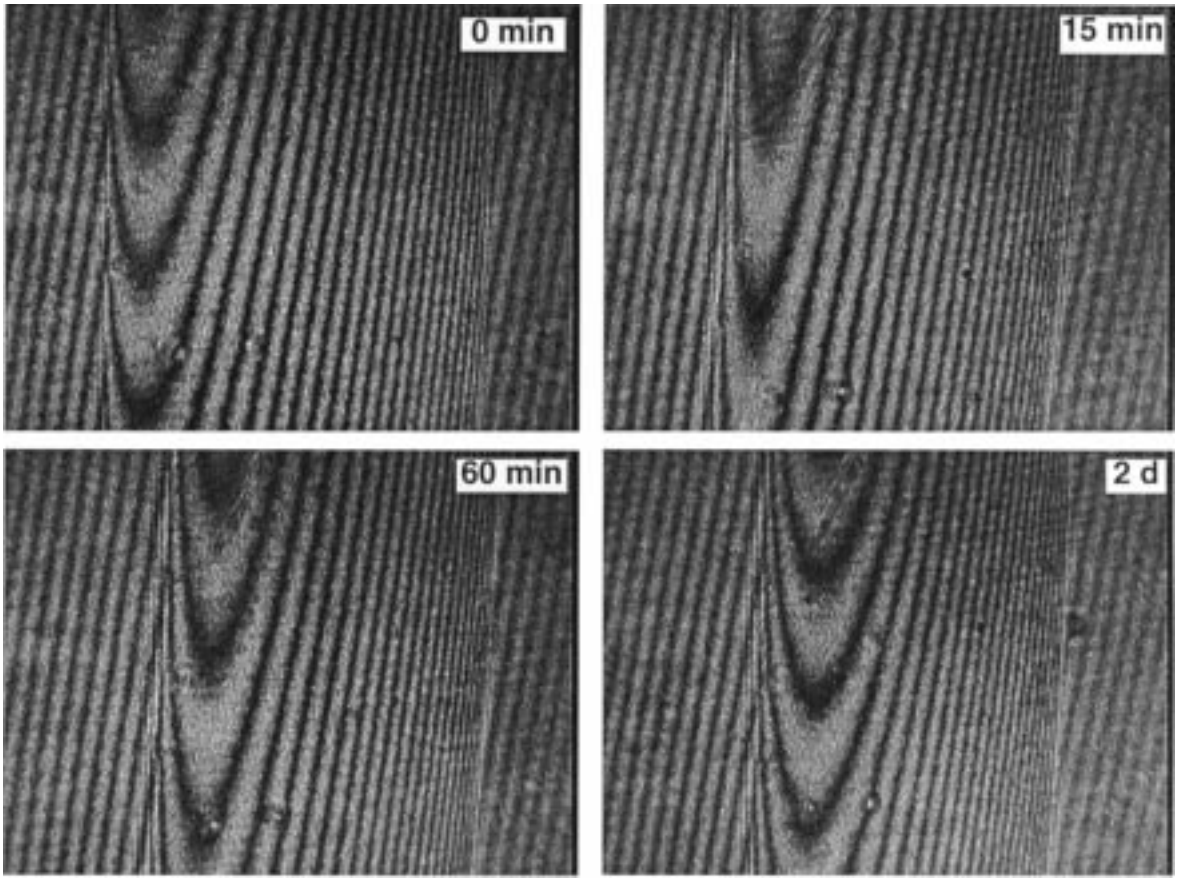

Figure 4. Examples of gel interferograms for a PAAm gel deswelling in a solution of 25 wt % methanol in water at four different times. Initially (0 min), the gel was in pure water.

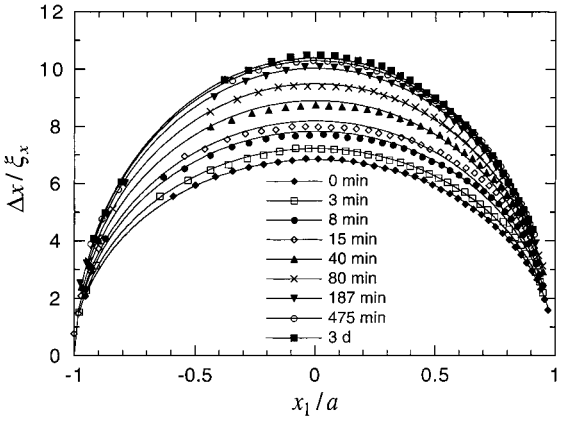

Figure 5. Relative displacement $\Delta x/\xi_x$ plotted as a function of the fringe position for a PAAm gel deswelling in a solution of 25 wt % methanol in water at different times. The time is indicated in the legend. Lines are the best fit by semiellipses.

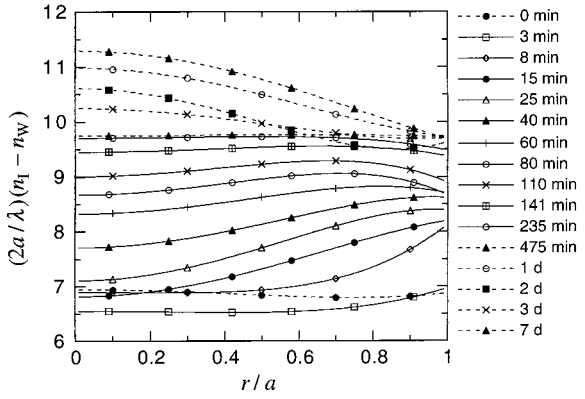

Figure 6. Change in the refractive index profile in the deswelling.

than sufficient to offset the decrease in $2a$. The fitting is good for 0, 80, 187, and 475 min but poor for the other plots. From 3 to 40 min, the center portion is more depressed relative to the fitting curve of an ellipse, whereas the edge portion runs higher. For the 3 day plot, in contrast, the center runs higher.

By deconvoluting the displacement plots with eqs 5−7 with $N = 2$, the plots were converted into those of $(2a/\lambda)[n_I(r) - n_E]$. Deconvolution with $N = 3$ or 4 produced similar plots, only to emphasize errors, and therefore were not used. The deconvolution plots thus obtained are with reference to the 25 wt % solution of methanol except for the 0 min plot which is with reference to pure water. To convert the plots to those with reference to water, we used $n_E - n_W = 0.250 \times (-0.00155) = -3.87 \times 10^{-4}$. The converted plots are shown in Figure 6.

At time $t = 0$ min (water-swollen gel), $n_I(r)$ is close to flat, indicating that the gel matrix is nearly uniform with $c_G = 0.0230$ g/mL. In 3 min, the refractive index dropped almost uniformly except for the edge portion which showed a slightly higher index. Afterward, the index started to increase from the edge, followed by an increase at the center of the gel. At 187, 235, and 475 min, the profile was again nearly flat. The profiles at 235, 321 (not shown), and 475 min were almost identical. From 235 to 475 min, the gel density was almost flat at $c_G = 0.0391$ g/mL. We found, however, that afterward the gel developed nonuniformness with a higher density at the center. The profiles increased in 1 day, then decreased in 2 and 3 days, and finally

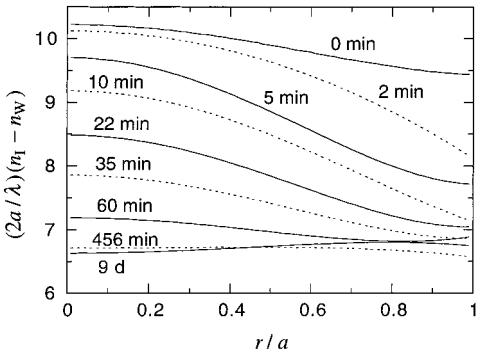

Figure 7. Change in the refractive index profile in the reswelling.

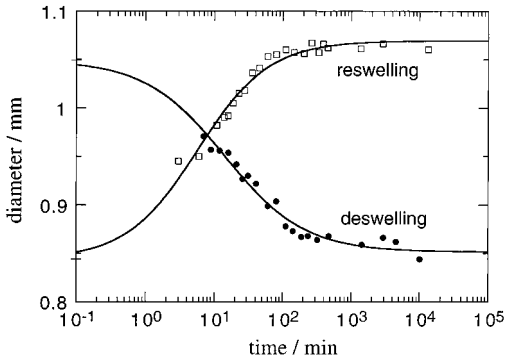

Figure 8. Change in the diameter in the deswelling (closed circles) and reswelling (open squares) processes. See text for the curve fitting.

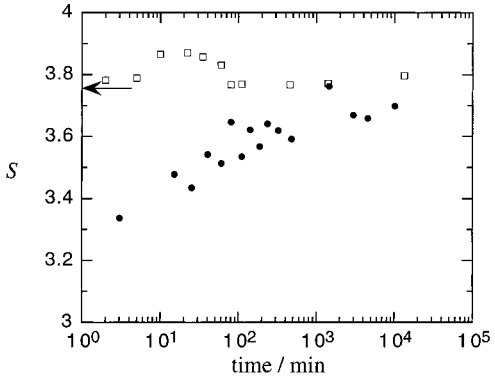

Figure 9. Plot of S as a function of time time in the deswelling (closed circles) and reswelling (open squares). The arrow indicates the original value of S before deswelling.

increased again in 7 days. During this late-stage change, the edge portion barely changed its density. We do not know whether this change is periodical or not; the frequency of image recording was not sufficient. It is not certain either whether the gel reached equilibrium in 7 days or not.

The initial drop in $n_I - n_S$ as seen in the 3 min plot may be ascribed to the change in the temperature of the surrounding solution when it was transferred from another cell at 25.0 °C to the measurement cell via a glass pipet; the pipet was left at room temperature. A temporary hike in the temperature makes n_E smaller, causing $n_I - n_E$ to rise. A lower temperature causes $n_I - n_E$ to drop. A temperature drop needed for an increase of 0.4 in $(2a/\lambda)n_E$ is estimated to be less than 2 K, where dn/dT values of water and methanol were used for the estimate. The temperature should have returned to 25.0 °C in less than 10 min, considering the quick response of the cell temperature upon change of the temperature in the circulating water. Another possibility of the initial drop is that, when the edge starts to contract, it may accompany the expansion of the center.

The pattern of change in $n_I(r)$ is remarkable. It took a long time for the edge of the hydrogel to reach equilibrium, nearly as long as the time needed for the center portion. The increase in the gel density was rather close to uniform from the center to the edge. We note that use of $N = 3$ or 4 in the deconvolution resulted in a similar profile change. This observation does not agree with theoretical models for a volume change of a cylindrical gel with a zero shear modulus. In the absence of the shear modulus, the edge portion would establish the equilibrium upon change of the surrounding fluid.[13−15] Apparently, the edge was constrained by the yet relaxing center portion of the gel to maintain its integrity. The result indicates that the gel studied had a shear modulus comparable to the bulk modulus.[15]

We also studied kinetics of reswelling in the interferometry. After the last recording in the deswelling experiment, the exterior solution was replaced by pure water. The surrounding water was changed frequently. The interferograms and the diameter were recorded at different times as the gel reswelled. The refractive index profiles are shown in Figure 7. In 2 min, the refractive index of the edge portion dropped compared to the original methanol mixture-equilibrated gel (0 min). The gel matrix expanded from the edge. The rate of decrease in the gel density was similar between the edge and the center until 22 min after the solvent change, although the center portion maintained a higher density. In 60 min, the gel almost regained its uniformness, followed by further homogeneous swelling. After being swollen in water for 9 days, the gel developed a slight nonuniformness with a higher density near the edge. Also, the gel at this time had a lower refractive index compared to the value when it was originally swollen in water (see the 0 min plot in Figure 6). It may be ascribed to a partial damage on the gel matrix during the deswelling and reswelling processes.

The self-diffusion coefficients of water and methanol at 25 °C are 2.4×10^{-5} and 2.3×10^{-5} cm^2/s, respectively.[31] Then the time required for the fluid within the gel to become identical to the surrounding fluid is estimated to be just a minute in both deswelling and swelling. It took a much longer time for the gel matrix to relax, in agreement with the reported experimental results.[1]

Diameter Change. The changes in the diameter d of the gel with time t during the deswelling and reswelling are shown in Figure 8. In the deswelling, the diameter decreased gradually and stabilized in almost 3 h in agreement with the density profile change. When the exterior solution was exchanged to pure water, the diameter increased. The equilibrium diameter exceeded that of the original water-swollen gel, again in agreement with the interferometry results. The following equation was used for the curve fitting of the diameter change:

$$d = d_i + \Delta d[1 + \tanh(\beta \ln (t/\tau))] \qquad (9)$$

where d_i is the diameter at $t = 0$, Δd is the overall change in d, τ is characteristic time of the change, and β indicates the spread in the time scale for the change. A greater β means that the change occurred in a shorter span of time. In the curve fitting, the actual measured

value was used for d_i (1.049 mm for deswelling and 0.844 mm for reswelling), and the other three parameters were used to minimize the squared difference between the data and the fitting equation. The fitting yielded $\beta = 0.374$ and $\tau = 14.42$ min for the deswelling and $\beta = 0.420$ and $\tau = 5.76$ min for the reswelling. The volume change was slower and more diffuse in the deswelling compared with the reswelling. This difference also attests a large deformation in our experiments that may have exceeded the linear response regime.

Isotropic Deformation. When a cylindrical gel of diameter $d = 2a$ and length L deforms while maintaining the overall shape, $L\int_0^a rc_G(r)\,dr$ should be held constant. If a and L keep their proportion in the deformation, then

$$S \equiv d^2\int_0^1 x(2a/\lambda)[n_I(ax) - n_W]\,dx \qquad (10)$$

should not change. Figure 9 is a plot of S in deswelling and reswelling. In the deswelling, S dropped initially from the value for the water-swollen gel (indicated by the arrow) and then climbed back slowly to the original value, indicating that the lateral contraction was faster than longitudinal contraction. The smaller dimension is more sensitive to the environmental change. In swelling, however, S maintained nearly unchanged except for a small increase at short times.

Concluding Remarks

In this paper, we have shown that the interferometric imaging can provide the density profile for the matrix of a hydrogel that is deswelling in a poorer solvent condition and reswelling in pure water. The profile started to change from the edge and proceeded to the center. The edge of the gel did not establish equilibrium immediately after the solvent change, however, indicating a large shear modulus. To study the volume changes more closely, we are currently applying the imaging technique to study of deswelling in smaller changes in the methanol content, from 10 to 15 wt %, for instance. Preliminary results indicate a profile change similar to the one we observed here.

The structural changes of gels are not limited to those caused by a change in the interaction between solvent and the gel matrix. An aqueous solution of polymer can also shrink the hydrogel because of its osmotic pressure. In particular, when the polymer has a high molecular weight and cannot easily penetrate the gel matrix, the refractive index profile reflects purely the gel matrix. The imaging will not be compromised by simultaneous infusion of polymer chains. Unlike our present study, transfer of water directly causes contraction of the gel matrix at the same time. The mechanism of the volume change will be different.

Acknowledgment. We thank T. K. Kwei for helpful discussion. We acknowledge the support by NSF Grant DMR-9458055.

References and Notes

(1) Gehrke, S. H. In *Responsive Gels: Volume Transitions II*; Duošek, K., Ed.; Springer: Berlin, 1993; Vol. 110.
(2) Tanaka, T.; Fillmore, D. J.; Sun, S.; Nishio, I.; Swislow, G.; Shah, A. *Phys. Rev. Lett.* **1980**, *45*, 1636.
(3) Tanaka, T.; Ishikawa, S.; Ishimoto, C. *Phys. Rev. Lett.* **1977**, *38*, 771.
(4) Tanaka, T. *Phys. Rev. Lett.* **1978**, *40*, 820.
(5) Tanaka, T.; Sato, E.; Hirokawa, Y.; Hirotsu, S. *Phys. Rev. Lett.* **1985**, *55*, 2455.
(6) Joosten, J. G. H.; McCarthy, J. L.; Pusey, P. N. *Macromolecules* **1991**, *24*, 6690.
(7) Shibayama, M.; Fujikawa, Y.; Numura, S. *Macromoleucles* **1996**, *29*, 6535.
(8) Shibayama, M. In *Structure and Properties of Multiphase Polymeric Materials*; Araki, T., Tran-Cong, Q., Shibayama, M., Eds.; Marcel Dekker: New York, 1998.
(9) Shibayama, M. *Macromol. Chem. Phys.* **1998**, *199*, 1.
(10) Sato Matsuo, E.; Tanaka, T. *J. Chem. Phys.* **1988**, *89*, 1695.
(11) Hu, Y.; Horie, K.; Ushiki, H.; Tsunomori, F.; Yamashita, T. *Macromolecules* **1992**, *25*, 7324.
(12) Ikehara, T.; Nishi, T.; Hayashi, T. *Polym. J.* **1996**, *28*, 169.
(13) Tanaka, T.; Fillmore, D. J. *J. Chem. Phys.* **1979**, *70*, 1214.
(14) Li, Y.; Tanaka, T. *J. Chem. Phys.* **1990**, *92*, 1365.
(15) Wang, C.; Li, Y.; Hu, Z. *Macromolecules* **1997**, *30*, 4727.
(16) Tanaka, H.; Tomita, H.; Takasu, A.; Hayashi, T.; Nishi, T. *Phys. Rev. Lett.* **1992**, *68*, 2794.
(17) Sato Matsuo, E.; Tanaka, T. *Nature* **1992**, *358*, 482.
(18) Barrière, B.; Sekimoto, K.; Leibler, L. *J. Chem. Phys.* **1996**, *105*, 1735.
(19) Dube, A.; Teraoka, I. *Macromolecules* **1997**, *30*, 5352.
(20) Yasunaga, H.; Kurosu, H.; Ando, I. *Macromolecules* **1992**, *25*, 6509.
(21) Ilg, M.; Pfleiderer, B.; Albert, K.; Rapp, W.; Bayer, E. *Macromolecules* **1994**, *27*, 2778.
(22) Shibuya, T.; Yasunaga, H.; Kurosu, H.; Ando, I. *Macromolecules* **1995**, *28*, 4377.
(23) Ahuja, S.; Dieckman, S. L.; Gopalsami, N.; Raptis, A. C. *Macromolecules* **1996**, *29*, 5356.
(24) Fyfe, C. A.; Blazek, A. I. *Macromolecules* **1997**, *30*, 6230.
(25) Hyde, T. M.; Gladden, L. F. *Polymer* **1998**, *39*, 811.
(26) Schlick, S.; Pilar, J.; Kweon, S.-C.; Vacik, J.; Gao, Z.; Labsky, J. *Macromolecules* **1995**, *28*, 5780.
(27) Gao, Z.; Pilaoř, J.; Schlick, S. *J. Phys. Chem.* **1996**, *100*, 8430.
(28) Teraoka, I. *Macromolecules* **1996**, *29*, 2430.
(29) Xu, Y. Thesis, Polytechnic University, 1999.
(30) http://www.ampolymer.com/light.htm.
(31) Levine, I. N. *Physical Chemistry*, 4th ed.; McGraw-Hill: New York, 1995.

MA990261X